Sonodynamically-induced apoptosis, necrosis, and active oxygen generation by mono-l-aspartyl chlorin e6

Nagahiko Yumita,[1,3] Qing-Song Han,[1] Ikuko Kitazumi[1] and Shin-ichiro Umemura[2]

[1]School of Pharmaceutical Sciences, Toho University, 2-2-1 Miyama, Funabashi, Chiba 274-8510; [2]Department of Electrical and Communication Engineering, Tohoku University, Aoba 6-6-05, Aramaki, Aoba-ku, Sendai 980-8579, Japan

(Received May 28, 2007/Revised September 20, 2007/Accepted September 20, 2007/Online publication October 29, 2007)

In this study, we investigated the induction of apoptosis by ultrasound in the presence of a photochemically active chlorine, mono-l-aspartyl chlorin e6 (NPe6). HL-60 cells were exposed to ultrasound for up to 3 min in the presence and absence of NPe6, and the induction of apoptosis was examined by analyzing cell morphology, DNA fragmentation, and caspase-3 activity. Cells treated with 80 μM NPe6 and ultrasound clearly showed membrane blebbing and cell shrinkage, whereas significant morphologic changes were not observed in cells exposed to either ultrasound alone, at the same intensity, or NPe6 alone. Also, DNA ladder formation and caspase-3 activation were observed in cells treated with both ultrasound and NPe6 but not in cells treated with ultrasound or NPe6 alone. In addition, NPe6 substantially enhanced nitroxide generation by ultrasound in the same acoustical arrangement. Sonodynamically-induced apoptosis, caspase-3 activation, and nitroxide generation were significantly suppressed by histidine. These results suggest that the combination of ultrasound and NPe6 sonochemically induces apoptosis as well as necrosis in HL-60 cells. They further suggest that some ultrasonically-generated active species, deactivatable by histidine, are the major mediators to induce the observed apoptosis. (*Cancer Sci* 2008; 99: 166–172)

Ultrasound has a tissue attenuation coefficient that allows it to penetrate intervening tissues and reach internal targets without losing the ability to focus energy into small volumes. This is a unique advantage over electromagnetic modalities such as laser light and microwaves for the non-invasive treatment of internal tumors. Although the use of ultrasound for tumor treatment has been well investigated with respect to the thermal effects of ultrasound absorption,[1,2] only a few groups have reported its non-thermal effects, such as potential sonochemical effects.[3–7]

Recently, we found that some photochemically active porphyrins, such as hematoporphyrin and porfimer sodium,[8,9] are also sonochemically active and therefore can induce significant cell damage when activated by ultrasound.[10–14] When implanted murine tumors are treated after the such chemicals are given, tumor growth is significantly inhibited at an intensity where ultrasound alone shows only a slight inhibitory effect.[15,16] Therefore, photochemically active porphyrins might be useful for sensitizing tumors to ultrasound. We have proposed that this potential modality should be called "sonodynamic therapy".[11,17]

Mono-l-aspartyl chlorin e6 (NPe6; Fig. 1) shows a much longer phosphorescence lifetime than porfimer sodium or hematoporphyin derivative.[18] This long phosphorescence lifetime can be a great advantage for the efficient photochemical generation of singlet oxygen. It has been reported that NPe6 is much less toxic than porfimer sodium. In mice, the lethal dose of NPe6 is much higher than that of porfimer sodium. These can be the advantages of NPe6 over porfimer sodium in sonodynamic as well as photodynamic treatments. Furthermore, like some porphyrins, NPe6 is preferentially retained by tumor tissues. Gomer and Ferrario showed that NPe6 accumulated in colon 26 tumor tissue after intravenous injection, allowing significant destruction of the tumor tissue on irradiation with pulsed laser light, suggesting that NPe6 is an effective photosensitizer for use in photodynamic therapy.[19]

Apoptosis can be initiated by a wide variety of intracellular and extracellular stimuli and is a mechanism for the removal of unnecessary, aged, or damaged cells. Cells undergoing apoptosis show characteristic morphological changes, including initial shrinkage, followed by widespread membrane blebbing, chromatin condensation, and DNA fragmentation. The cell further disassembles into membrane-enclosed vesicles called apoptotic bodies that are rapidly taken up and digested by neighboring cells and phagocytes.[20–22]

Recently, ultrasonic exposure has been shown to trigger apoptosis in both normal and malignant cells. Ultrasound-induced apoptotic cell death has been confirmed in K562, HL-60, and U937 leukemia cells.[23–27] In addition, contrast agents are reported to enhance ultrasonically-induced apoptosis.[28] In this study, we examined the effect of NPe6 on ultrasonically-induced apoptosis as well as the mechanism behind it.

Materials and Methods

Chemicals. NPe6 was a generous gift from Meiji Seika Kaisha (Tokyo, Japan). Trypan blue, agarose, RNase A, and proteinase K were purchased from Wako (Tokyo, Japan). Histidine, superoxide dismutase (SOD), mannitol, ethidium bromide, 2,2,6,6-tetramethyl-4-piperidone (TMPone), 2,2,6,6-tetramethyl-4-piperidone-N-oxyl, 2,2,6,6-tetramethyl-4-piperidol-N-oxyl sodium azide (NaN_3), butylated hydroxytoluene (BHT) and diphenylamine were purchased from Sigma Aldrich (St. Louis, MO, USA). All other reagents were of analytical grade.

Cell culture. Human promyelocytic leukemia HL-60 cells were obtained from the Riken Gene Bank (Tokyo, Japan). Cells were maintained in RPMI-1640 medium supplemented with 10% heat-inactivated fetal bovine serum (Gibco BRL, Tokyo, Japan), 100 U/mL penicillin G, 100 μg/mL streptomycin, and 2 mM glutamine (Sigma Aldrich) in an atmosphere of 5% CO_2 in humidified air at 37°C.

Ultrasound apparatus. The apparatus for ultrasonic exposure is shown schematically in Fig. 2. The ultrasound transducer uses a piezoelectric ceramic disk 24 mm in diameter and was driven at its resonance frequency (1.93 MHz). Before exposure, the HL-60 cells were harvested, washed twice in phosphate-buffered saline (PBS, pH 7.4), resuspended at a concentration of 1×10^6 cells/mL in 2.5 mL of RPMI-1640 (serum free), and transferred into a

[3]To whom correspondence should be addressed.
E-mail: nagahiko@phar.toho-u.ac.jp

doi: 10.1111/j.1349-7006.2007.00653.x

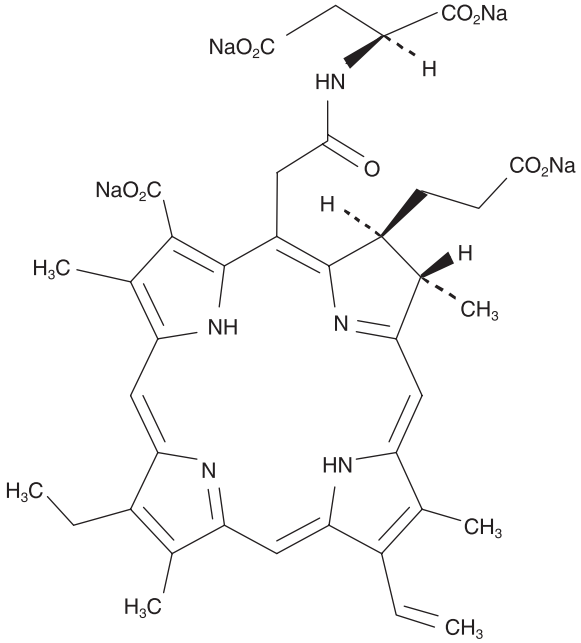

Fig. 1. Chemical structure of mono-l-aspartyl chlorin e6 (NPe6).

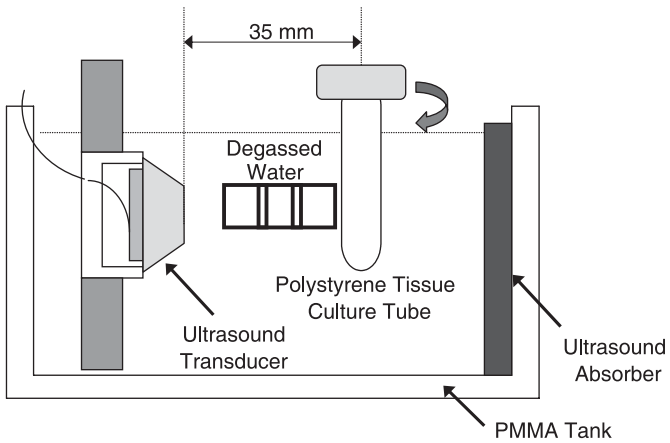

Fig. 2. Diagram of the ultrasonic exposure apparatus used in this experiment.

cylindrical 16 × 125 mm polystyrene tissue culture tube (Corning, Corning, NY, USA). The polystyrene tissue culture tube was suspended 35 mm away from the surface of the plane-wave transducer in degassed water, and exposed to ultrasound at 37°C. Immediately before exposure, NPe6 was added to the cell suspension. During exposure, the tube was rotated at 60 r.p.m. by a synchronous motor to improve mixing and to provide a uniform exposure. The cells were exposed to ultrasound for up to 3 min in the presence and absence of NPe6. The samples treated with NPe6 alone were kept in the same position for the same period as the ultrasonic exposure. Ultrasonic output from the transducer was evaluated in degassed water by placing the axis of the transducer horizontally. The output acoustic power was calibrated by measuring the radiation force on a 2-mm-thick hollow aluminum plate with an area of 20 × 28 mm, suspended at an angle of 45° to the axis. Its horizontal projection was therefore 20 mm × 20 mm. The ultrasonic intensity was calculated by dividing the measured acoustic power by the projected area. The temperature rise in 2.5 mL RPMI-1640 in the container during a 5-min exposure at the highest ultrasonic intensity used in the experiments was less than 1°C. After the treatment procedure, the medium was replaced with fresh RPMI-1640 with 10% fetal bovine serum and the cells were incubated in an atmosphere humidified with 5% CO_2 at 37°C for 6 h before the cell viability and apoptotic fraction were measured.

Evaluation of cell damage and apoptosis. Apoptosis is characterized by morphological changes such as membrane blebbing, cell shrinkage, and disassembling into apoptotic bodies. After the treatment, HL-60 cells were examined using a phase contrast inverted microscope (Olympus, Japan) at ×400 magnification. The viability of the treated cells was determined by staining of the cells with Trypan blue immediately after the treatment. The fraction of apoptotic cells was determined by counting the number of unstained cells showing morphological changes on a hemocytometer glass plate. The integrity was checked right before each series of treatment, and cell suspensions with integrity above 99% were used. This number of intact cells before treatment was regarded as the standard for the integrity determination after each treatment.

Electrophoretic analysis of DNA fragmentation. After the incubation following each treatment, the cells were harvested, washed in PBS (pH 7.4) then lyzed in 100 μL of 0.1 M phosphate–citrate buffer solution. Following lysis, the samples were centrifuged at 16 000*g* for 5 min. Then supernatants were processed with 200 μg/mL DNase-free RNase (2 μL) at 37°C for 1 h, followed by a process with 1 μg/mL proteinase K (1 μL) at 50°C for 1 h. The samples were electrophoresed at 50 V for 3 h in 1.5% (w/v) agarose gels complemented with 1 μg/mL ethidium bromide. Separated DNA fragments (DNA ladders) were visualized using an ultraviolet transilluminator. The size of DNA fragments was determined by comparison with DNA molecular weight markers (*Hin*dIII DNA; Invitrogen, USA).

Measurement of caspase-3 activity. Caspase-3 activity was assayed using the specific fluorogenic substrate Ac-DEVD-AFC (MBL, Tokyo, Japan). Treated cells were washed with 50 mM PBS (pH 7.4) then resuspended in buffer containing 50 mM Tris-HCL (pH 7.4), 1 mM ethylenediaminetetraacetic acid (EDTA), and 10 mM ethyleneglycoltetraacetic acid (EGTA). The cell lysates were then centrifuged at 800*g* for 5 min, and the supernatant was incubated with 50 μM of peptide substrate at 37°C for 2 h. The formation of 7-amino-4-trifluoromethylcoumarin was measured using a fluorescence spectrophotometer (F-3000; Hitachi, Japan) with excitation at 400 nm and emission at 505 nm. The enzyme activity measured just prior to each experiment was used as the control. The caspase activity was expressed as the ratio of released 7-amino-4-trifluoromethylcoumarin for the experimental condition compared to the untreated control.

Electron spin resonance (ESR) measurements. Ultrasonically-induced nitroxide production in the presence and absence of NPe6 was measured by ESR spectroscopy in an air-saturated aqueous solution of 50 mM TMPone in the presence and absence of oxygen scavengers. The pH of the solutions was adjusted to 9.0 with 50 mM PBS. At appropriate time points, samples were taken for ESR measurement and placed in glass capillary tubes with an inner diameter of 1.1–1.2 mm, a wall thickness of 0.2 mm, and a length of 75 mm (Allied Corporation Fisher Scientific, Pittsburgh, PA, USA). The ESR spectra were recorded using a JEOL JES-FE3XG X-band spectrometer (JEOL, Tokyo, Japan) operating at a 100 kHz modulation frequency and at a 9.26 GHz microwave frequency. The modulation amplitude of the magnetic field was set at 1.0×10^{-4} T, and the microwave power was 10 mW. The concentration of the produced nitroxide was determined by comparison with the peak-to-peak ESR signal amplitude of a 1 mM 2,2,6,6-tetramethyl-4-piperidone-N-oxyl solution. The ratio of the amplitude to the nitroxide

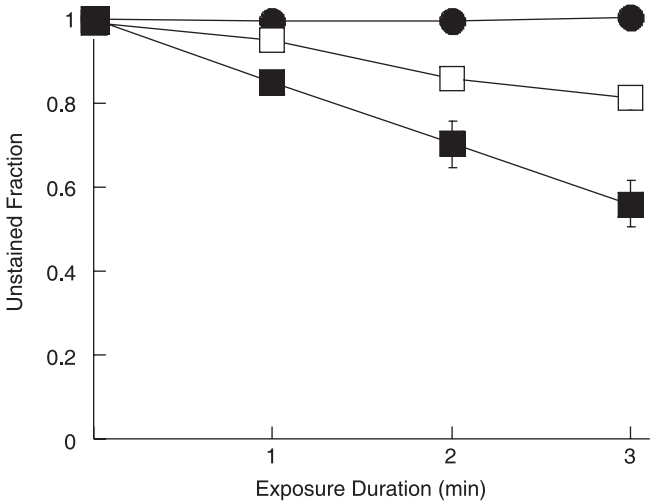

Fig. 3. Fraction of human promyelocytic leukemia HL-60 cells not stained with Trypan blue following ultrasonic exposure in the presence and absence of mono-l-aspartyl chlorin e6 (NPe6). (● 80 μM NPe6 alone; (□) ultrasound alone; (■) 80 μM NPe6 + ultrasound. Values represent the means ± standard deviation of four independent experiments.

concentration was also verified by comparison with the peak-to-peak ESR signal amplitude of a 1 mM 2,2,6,6-tetramethyl-4-piperidol-N-oxyl solution.

Statistical analysis. The results were expressed as the mean ± standard deviation. The values were compared by Student's *t*-test with 0.05 as the minimum level of significance.

Results

Cell damage. We first exposed HL-60 cells to ultrasound at 6 W/cm^2 in the presence and absence of 80 μM NPe6 and examined their integrity by staining with Trypan blue. Fig. 3 shows the fraction of unstained HL-60 cells versus the duration of exposure. The results show that the unstained (intact) fraction decreased exponentially with the duration of exposure. Following exposure to ultrasound for 3 min in the presence and absence of NPe6, the fraction of unstained cells was 80% and 56%, respectively. NPe6 alone did not cause cell damage.

Morphological changes. We next assessed the induction of apoptosis by examining the morphology of the cells with a phase contrast microscope after a 4-h incubation with no addition, 80 μM NPe6 alone, ultrasound alone (6 W/cm^2), and ultrasound at the same intensity in the presence of NPe6. There was no significant morphological change in the cells treated with either NPe6 alone (Fig. 4b) or ultrasound alone (Fig. 4c). In contrast, the combination of ultrasound and NPe6 clearly caused membrane blebbing and cell shrinkage (Fig. 4d).

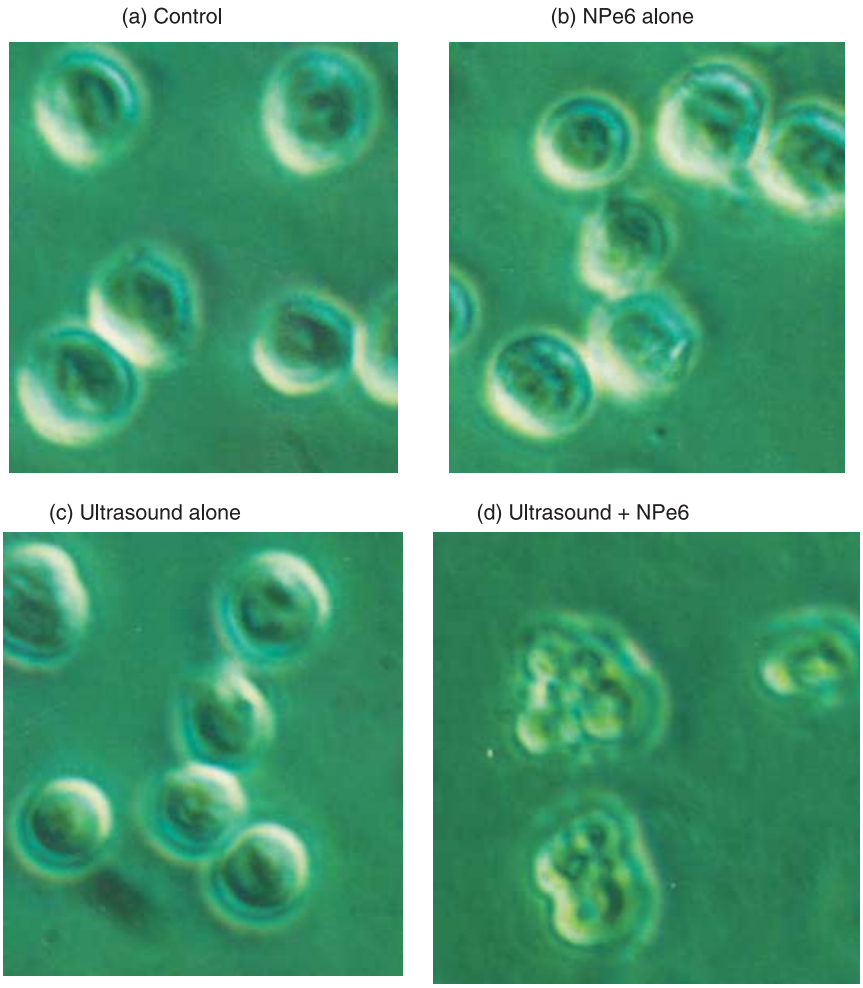

Fig. 4. Analysis of cellular morphology of human promyelocytic leukemia HL-60 cells by phase contrast microscopy after a 4-h incubation under the following conditions: (a) control; (b) 80 μM mono-l-aspartyl chlorin e6 (NPe6) alone; (c) ultrasound alone; and (d) 80 μM NPe6 + ultrasound.

doi: 10.1111/j.1349-7006.2007.00653.x

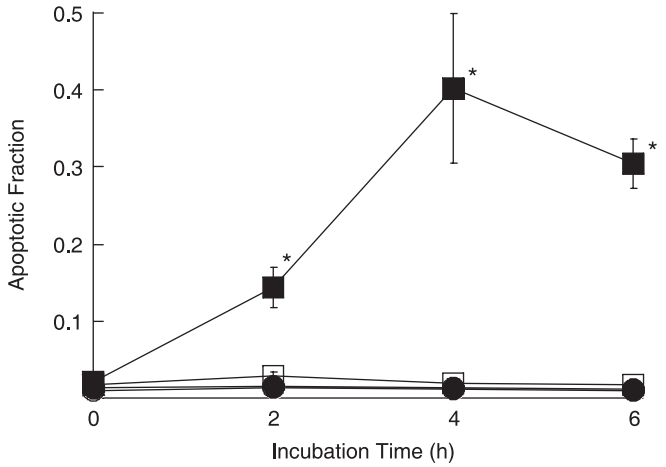

Fig. 5. Fraction of apoptotic human promyelocytic leukemia HL-60 cells after 3-min exposure to ultrasound in the presence and absence of mono-l-aspartyl chlorin e6 (NPe6). (○) control; (●) 80 μM NPe6 alone; (□) ultrasound alone; (■) 80 μM NPe6 + ultrasound. Values represent the means ± standard deviation of four independent experiments. $*P < 0.05$ versus untreated control. The values of the control were similar to those of NPe6 alone.

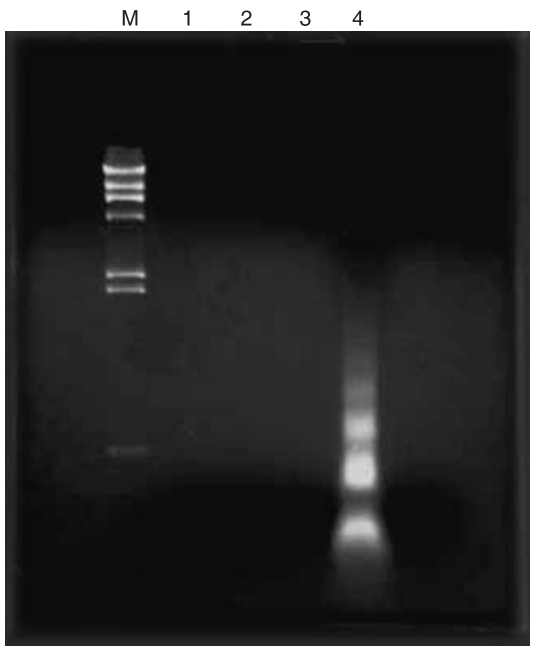

Fig. 6. DNA ladder formation in human promyelocytic leukemia HL-60 cells 4 h after exposure to mono-l-aspartyl chlorin e6 (NPe6) and/or ultrasound. M, DNA size markers; 1, control; 2, 80 μM NPe6 alone; 3, ultrasound alone; 4, 80 μM NPe6 + ultrasound.

Induction of apoptosis. From the phase contrast microscope images, we calculated the fractions of apoptotic cells and plotted them versus time (Fig. 5). Under all conditions, the fraction of apoptotic cells was less than 2% immediately following initiation of the treatment. In cells exposed to ultrasound in the presence of NPe6, there was a significant increase in the fraction of apoptotic cells that increased with time. The fraction of apoptotic cells reached a maximum after 4 h and then decreased. A significant increase in the apoptotic fraction was not observed in cells exposed to ultrasound at the same intensity or NPe6 alone.

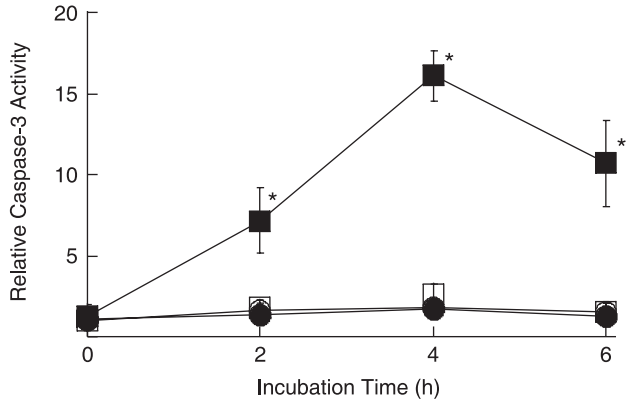

Fig. 7. Caspase-3 activity in human promyelocytic leukemia HL-60 cells after 3-min exposure to ultrasound in the presence and absence of mono-l-aspartyl chlorin e6 (NPe6). The ratios of the activity to untreated cells are plotted. (○) control; (●) 80 μM NPe6 alone; (□) ultrasound alone; (■) 80 μM NPe6 + ultrasound. Values represent the means ± standard deviation of four independent experiments. $*P < 0.05$ versus untreated cells. The values of the control were similar to those of NPe6 alone.

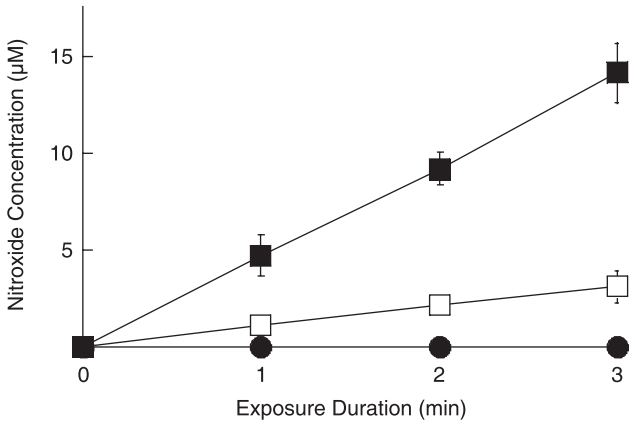

Fig. 8. Nitroxide generation in an air-saturated solution of 50 mM 2,2,6,6-tetramethyl-4-piperidone during exposure to ultrasound in the presence and absence of mono-l-aspartyl chlorin e6 (NPe6). (○) control; (●) 80 μM NPe6 alone; (□) ultrasound alone; (■) 80 μM NPe6 + ultrasound. Values represent the means ± standard deviation of four independent experiments. $*P < 0.05$ versus untreated control. The values of the control were similar to those of NPe6 alone.

DNA fragmentation. To further explore the induction of apoptosis, we carried out agarose gel electrophoresis of DNA samples from the HL-60 cells (Fig. 6). A characteristic DNA ladder in HL-60 cells was observed 4 h after the exposure to ultrasound in the presence of 80 μM NPe6 (lane 4). An obvious DNA ladder was not observed in cells exposed to either ultrasound (lane 2) or NPe6 alone (lane 3).

Caspase-3 activation. To investigate whether caspases are activated by sonodynamic treatment in HL-60 cells, we measured the enzymatic activity of caspase-3 using a fluorescent peptide substrate (Fig. 7). We found that the activity of caspase-3 increased, reached a maximum after 4 h, then decreased in cells treated with ultrasound in the presence of 80 μM NPe6. An increase in caspase-3 activity was not observed in cells treated with either ultrasound or NPe6 alone.

Nitroxide generation. The ESR and spin trapping techniques were carried out to determine whether active oxygen species including singlet oxygen and hydroxyl radicals participate in the induction of apoptosis by ultrasound. Fig. 8 shows the amounts

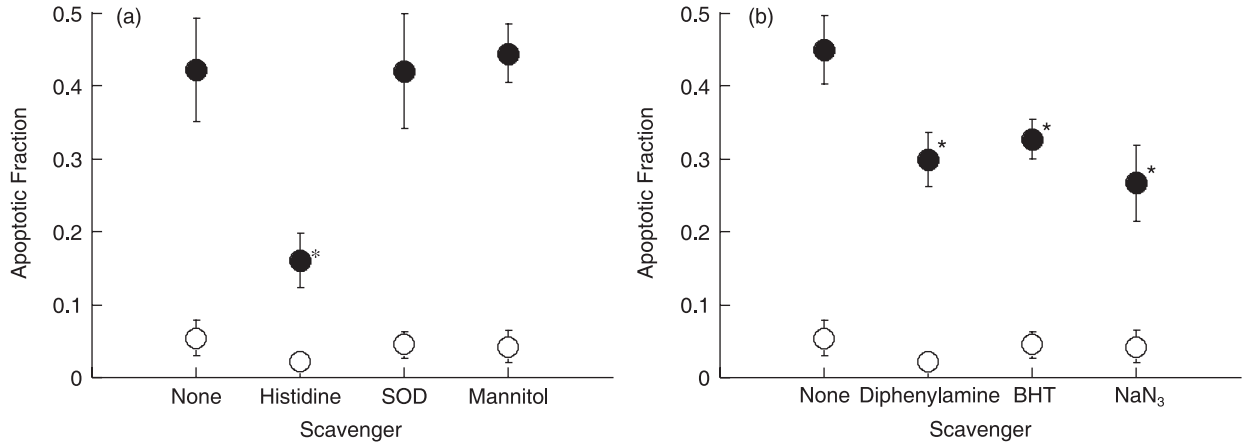

Fig. 9. Effect of active oxygen scavengers on ultrasonically-induced apoptosis in human promyelocytic leukemia HL-60 cells in the presence (●) and absence (○) of 80 μM mono-l-aspartyl chlorin e6. Values represent the means ± standard deviation of four independent experiments. *$P < 0.05$ versus no scavenger treatment.

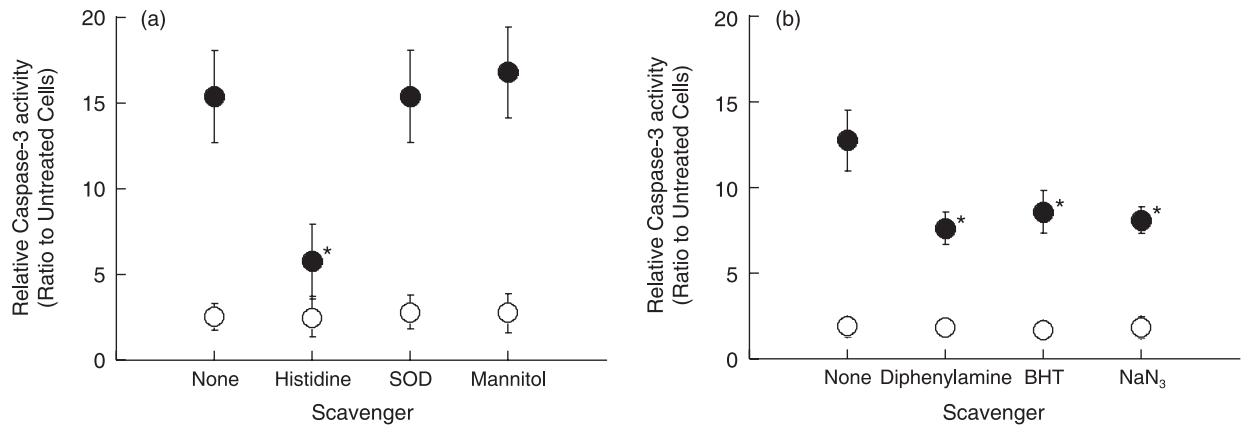

Fig. 10. Effect of active oxygen scavengers on ultrasonically-induced caspase-3 activation in the presence (●) and absence (○) of 80 μM mono-l-aspartyl chlorin e6. The ratios of the activity to untreated cells are plotted. Values represent the means ± standard deviation of four independent experiments. *$P < 0.05$ versus no scavenger treatment.

of nitroxide ultrasonically generated in air-saturated aqueous solutions of 50 mM TMPone with and without NPe6 under the same acoustic conditions as used in the cellular experiments. The nitroxide levels were determined from the ESR signal amplitudes and plotted versus the insonation time. The amount of ultrasonically-generated nitroxide increased linearly with the insonation time. NPe6 at a concentration of 80 μM enhanced the rate approximately threefold. Nitroxide generation was not observed with NPe6 alone.

Effect of active oxygen scavengers. To determine whether active oxygen species participate in the induction of apoptosis by ultrasound, we examined the effect of active oxygen scavengers (10 mM histidine, 100 μg/mL SOD, 100 mM mannitol, 50 mM diphenylamine, 50 mM BHT, and 5 mM NaN_3) on the fraction of cells showing morphological changes associated with apoptosis (Fig. 9), on the caspase-3 activity (Fig. 10), and on the production of nitroxide (Fig. 11). Histidine and NaN_3 significantly reduced the apoptosis induction, caspase-3 activation, and nitroxide generation, caused by exposure to ultrasound in the presence of NPe6. In contrast, SOD and mannitol did not effect these measurements at all. Diphenylamine and BHT significantly reduced the apoptotic induction and caspase-3 activity at 50 mM, but did not significantly reduce the nitroxide generation.

Discussion

In our initial morphological studies, we found that ultrasonically-induced apoptosis is greatly enhanced by NPe6. Specifically, we clearly observed membrane blebbing and cell shrinkage when cells were treated with a combination of ultrasound and NPe6, whereas significant morphologic changes were not observed in the cells exposed to either ultrasound or NPe6 alone. The fraction of apoptotic cells was significantly higher when they were treated with both ultrasound and NPe6 than with ultrasound alone or NPe6 alone. The fraction of stained cells shown in Fig. 3, which can be interpreted as necrotic cells, was also significantly higher for the combined treatment. These results suggest that sonodynamic activation of NPe6 induced apoptosis as well as necrosis.

The fragmentation of DNA at linker regions between nucleosomes into fragments that are multiples of 180–200 bp in length is a hallmark of apoptosis.[20] Using agarose gel electrophoresis, we found that ultrasonic exposure in the presence of NPe6 resulted in the formation of a characteristic DNA ladder. This was not observed immediately after exposure (data not shown) but was clear after 4 h incubation, indicating that DNA fragmentation was caused by an enzymatic process rather than by direct sonodynamic damage to the HL-60 cells.

doi: 10.1111/j.1349-7006.2007.00653.x

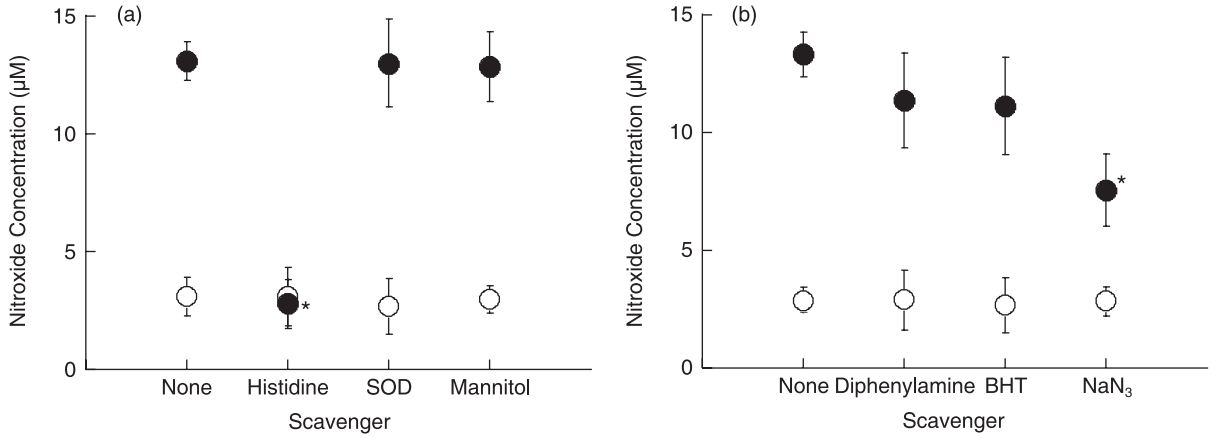

Fig. 11. Effect of active oxygen scavengers on ultrasonic nitroxide generation in the presence (●) and absence (○) of 80 μM mono-l-aspartyl chlorin e6. Values represent the means ± standard deviation of four independent experiments. *$P < 0.05$ versus no scavenger treatment.

Caspase-3 is an important enzyme required for the execution of the final phase of apoptosis, and it is active in cells undergoing apoptotic death.[22] We observed a significant activation of caspase-3 after treatment with a combination of ultrasound and NPe6. This activation of caspase-3 was associated with the induction of apoptosis. Both the apoptotic fraction and the activity of caspase-3 gradually increased to the maximum after 4 h then decreased, suggesting that caspase-3 acts as the executor caspase responsible for the induction of apoptosis by the combination treatment. Recently, plural pathways have been proposed for the activation of caspase-3 by photodynamic treatment.[21] A similar mechanism might also be involved in sonodynamically induced apoptosis. Further work will determine the mechanism of the sonodynamic activation of caspase-3.

The excited state of the sensitizer might be formed in the vicinity of collapsing ultrasonically-generated microbubbles in sonodynamic reactions.[29] Like photodynamic reactions, it might react with the substrates to generate free radicals. When the substrates contain oxygen, active oxygen species such as singlet oxygen might also be generated. We observed a substantial enhancement of nitroxide generation in the presence of NPe6 and under sonodynamic conditions used in the cellular experiments. Previous studies on the effects of active oxygen scavengers and D_2O substitution on sonodynamically-induced cell damage and on sonodynamic generation of active oxygen suggest that active oxygen species mediate the sonosensitizing effect of porphyrins.[11,14] We therefore examined the inhibitory effect of active oxygen scavengers on the fraction of sonodynamically-induced apoptotic cells, caspase-3 activation, and nitroxide generation.

Hiraoka *et al*. hypothesized that sonodynamically-induced cell killing was likely to be due to certain mechanical stress such as augmentation of physical disruption of cellular membrane by sensitizers.[30] However, the significant reduction by active oxygen scavengers such as histidine in both ultrasonically-induced apoptosis and caspase-3 activation clearly suggests that some ultrasonically-generated active species stimulated the apoptotic signaling pathways through caspase-3 activation.

The tested scavengers included: histidine, known to scavenge singlet oxygen and possibly hydroxyl radicals; 100 mM mannitol, a concentration that should scavenge both photodynamically and sonodynamically induced hydroxyl radicals;[13,31,32] and SOD, which catalyzes the elimination of superoxide radicals. Histidine caused a significant reduction in ultrasonically-induced apoptosis, caspase-3 activation, and nitroxide generation, suggesting that singlet oxygen is significantly more important than hydroxyl radicals or superoxide in the induction of apoptosis by ultrasound and NPe6.

Misik and Riesz suggest another possible mechanism of sonosensitizer-derived free radicals as mediators of sonodynamically induced cell damage.[33] They proposed that sonosensitization is due to the chemical activation of sonosensitizers in the close vicinity of hot collapsing cavitation bubbles to form sensitizer-derived free radicals. These carbon-centered free radicals react with oxygen to form peroxyl and alkoxyl radicals. In our experiments, diphenylamine (a scavenger of alkoxyl but not peroxyl radicals) and BHT (a scavenger of peroxyl radicals) each significantly decreased the apoptotic induction and caspase-3 activity.[34,35] Inhibitory effects of diphenylamine and BTH on ultrasonically-induced apoptosis and caspase-3 activation support their hypothesis. The overall results suggest that some active oxygen species, such as singlet oxygen and peroxyl and alkoxyl radicals, stimulate apoptotic signaling pathways through caspase-3 activation.

Histidine and NaN_3 can each potentially deactivate the excited state of NPe6, whereas neither mannitol nor superoxide dismutase can. Therefore, the effectiveness of histidine, NaN_3, diphenylamine, and BHT in contrast with the ineffectiveness of the other two can also be explained by the hypothesis that the observed sonodynamic enhancement of apoptosis by NPe6 was induced by reactive oxygen species such as singlet oxygen, and peroxyl and alkoxyl radicals. Singlet oxygen could be generated because the cell suspension was air-saturated in the ultrasonic exposure, at least when it was started.

In summary, we showed sonodynamically-induced apoptosis with NPe6 in HL-60 cells, as evidenced by morphological changes, DNA ladder formation, and caspase-3 activation. These results, as well as sonodynamically-induced necrosis with NPe6 in HL-60 cells, suggest the potential of NPe6 as a sonosensitizing agent for sonodynamic therapy. The significant reduction of sonodynamically-induced apoptosis and caspase-3 activation with NPe6 by histidine, NaN_3, diphenylamine, and BHT, and that of sonodynamically-induced nitroxide generation with NPe6 by histidine and NaN_3, indicate that some sonodynamically-generated active species, deactivatable by histidine, are the major mediators to induce the observed apoptosis.

References

1 Kremkau FW. Cancer therapy with ultrasound. *J Clin Ultrasound* 1979; **7**: 287.

2 Lele PP. Local hyperthermia by ultrasound. In: Nussbaum GH, ed. *Physical Aspects of Hyperthermia*. New York: American Institute of Physics, 1982; 393–440.

3 Rosenthal I, Sostaric ZJ, Riesz P. Sonodynamic therapy – a review of the synergistic effects of drugs and ultrasound. *Ultrason Sonochem* 2004; **11**: 349–63.
4 Yu T, Wang Z, Mason TJ. A review of research into the uses of low level ultrasound in cancer therapy. *Ultrason Sonochem* 2004; **11**: 95–103.
5 Umemura S, Kawabata K, Sasaki K, Yumita N, Umemura K, Nishigaki R. Recent advances in sonodynamic approach to cancer therapy. *Ultrason Sonochem* 1996; **3**: S187–91.
6 Tachibana K, Uchida T, Hisano S, Morioka E. Eliminating adult T-cell leukaemia cells with ultrasound. *Lancet* 1997; **349**: 9048.
7 Abe H, Kuroki M, Tachibana K *et al*. Targeted sonodynamic therapy of cancer using a photosensitizer conjugated with antibody against carcinoembryonic antigen. *Anticancer Res* 2002; **22**: 1575–80.
8 Bellnier DA, Ho YK, Panday RK, Missert JR, Dougherty TJ. Distribution and elimination of Photofrin II in mice. *Photochem Photobiol* 1989; **50**: 221–8.
9 Dougherty TJ. Photodynamic therapy. *Photochem Photobiol* 1993; **58**: 895–905.
10 Umemura S, Yumita N, Nishigaki R. Enhancement of ultrasonically induced cell damage by a gallium–porphyrin complex, ATX70. *Jpn J Cancer Res* 1993; **84**: 582–8.
11 Umemura S, Yumita N, Nishigaki R, Umemura S. Mechanism of cell damage by ultrasound in combination with hematoporphyrin. *Jpn J Cancer Res* 1990; **81**: 962–6.
12 Umemura K, Yumita N, Nishigaki R, Umemura S. Sonodynamically induced antitumor effect of pheophorbide a. *Cancer Lett* 1996; **102**: 151–7.
13 Yumita N, Nishigaki R, Sakata I, Nakajima S, Umemura S. Sonodynamically induced antitumor effect of 4-formyloximethylidene-3-hydroxy-2-vinyl-deuterio-porphynyl (IX)-6,7 diaspartic acid (ATX-S10). *Jpn J Cancer Res* 2000; **91**: 255–60.
14 Yumita N, Umemura S, Nishigaki R. Ultrasonically induced cell damage enhanced by photofrin II: mechanism of sonodynamic activation. *In Vivo* 2000; **14**: 425–9.
15 Yumita N, Nishigaki R, Umemura S. Sonodynamically induced antitumor effect of photofrin II on colon 26 carcinoma. *Cancer Res Clin Oncol* 2000; **126**: 601–06.
16 Yumita N, Sasaki K, Umemura S, Nishigaki R. Sonodynamically induced antitumor effect of a gallium–porphyrin complex, ATX-70. *Jpn J Cancer Res* 1996; **87**: 310–16.
17 Yumita N, Umemura S. Sonodynamic therapy with photofrin II on AH130 solid tumor. Pharmacokinetics, tissue distribution and sonodynamic antitumoral efficacy of photofrin II. *Cancer Chemother Pharmacol* 2003; **51**: 174–8.
18 Spikes JD, Bommer JC. Photobleaching of mono-L-aspartyl chlorin e6 (NPe6): a candidate sensitizer for the photodynamic therapy of tumors. *Photochem Photobiol* 1993; **58**: 346–50.
19 Gomer CJ, Ferrario A. Tissue distribution and photosensitizing properties of mono-L-aspartyl chlorin e6 in a mouse tumor model. *Cancer Res* 1990; **50**: 3985–90.
20 Thompson CB. Apoptosis in the pathogenesis and treatment of disease. *Science* 1995; **267**: 1456–62.
21 Schemp CM, Simon-Haarhaus B, Termeer CC *et al*. Hypericin photo-induced apoptosis involves the tumor necrosis factor-related apoptosis-inducing ligand (TRAIL) and activation of caspase-8. *FEBS Lett* 2001; **493**: 26–30.
22 Vantieghem A, Assefa Z, Vandenabeele P *et al*. Hypericin-induced photosensitization of HeLa cells leads to apoptosis or necrosis. Involvement of cytochrome c and procaspase-3 activation in the mechanism of apoptosis. *FEBS Lett* 1998; **440**: 19–24.
23 Feril LB Jr, Kondo T, Takaya K, Riesz P. Enhanced ultrasound-induced apoptosis and cell lysis by a hypotonic medium. *Int J Radiat Biol* 2004; **80**: 165–75.
24 Feril LB Jr, Tsuda Y, Kondo T *et al*. Ultrasound-induced killing of monocytic U937 cells enhanced by 2,2′-azobis (2-amidinopropane) dihydrochloride. *Cancer Sci* 2004; **95**: 181–5.
25 Feril LB Jr, Kondo T, Ogawa R, Zhao QL. Dose-dependent inhibition of ultrasound-induced cell killing and free radical production by carbon dioxide. *Ultrason Sonochem* 2003; **10**: 81–4.
26 Ashush H, Rozenszajn LA, Blass M *et al*. Apoptosis induction of human myeloid leukemic cells by ultrasound exposure. *Cancer Res* 2000; **60**: 1014–20.
27 Lagneaux L, de Meulenaer EC, Delforge A *et al*. Ultrasonic low-energy treatment: a novel approach to induce apoptosis in human leukemic cells. *Exp Hematol* 2002; **30**: 1293–301.
28 Feril LB Jr, Kondo T, Zhao QL *et al*. Enhancement of ultrasound-induced apoptosis and cell lysis by echo-contrast agents. *Ultrasound Med Biol* 2003; **29**: 331–7.
29 Foote CS. Definition of type I and type II photosensitized oxidation. *Photochem Photobiol* 1991; **54**: 659.
30 Hiraoka H, Honda H, Feril LB Jr, Kudo N, Kondo T. Comparison between sonodynamic effect and photodynamic effect with photosensitizers on free radical formation and cell killing. *Ultrason Sonochem* 2006; **13**: 535–42.
31 Halliwell B, Gutteridge JMC. *Free Radicals in Biology and Medicine*, 3rd edn. New York: Oxford University Press, 1985.
32 Goldstein S, Czapski G. Mannitol as OH scavenger in aqueous solutions and biological systems. *Int J Radiat Biol* 1984; **46**: 725–9.
33 Misik V, Riesz P. Free radical intermediates in sonodynamic therapy. *Ann NY Acad Sci* 2000; **899**: 335–48.
34 Yeh SL, Yang TH, Huang CH *et al*. Exposure of calf thymus DNA to autoxidized β-carotene results in the formation of 8-oxo-deoxyguanosine. *Food Chem* 2003; **81**: 439–45.
35 Van der Zee J, Van Steveninck J, Koster JF *et al*. Inhibition of enzymes and oxidative damage of red blood cells induced by t-butylhydroperoxide-derived radicals. *Biochim Biophys Acta* 1989; **980**: 175–80.

doi: 10.1111/j.1349-7006.2007.00653.x